Int. J. Heat Mass Transfer. Vol. 23, pp. 1117–1126

0017–9310/80/0801–1117 $02.00/0

EXPERIMENTAL STUDY OF NATURAL CONVECTION IN A HORIZONTAL CYLINDER WITH DIFFERENT END TEMPERATURES

SHIGEO KIMURA and ADRIAN BEJAN
Department of Mechanical Engineering, University of Colorado, Boulder, CO 80309, U.S.A.

(*Received* 28 *January* 1980)

Abstract—The phenomenon of natural convection in a horizontal pipe with different end temperature was studied experimentally in a cylindrical cavity with the ratio (diameter)/(length) = 0.112. The Rayleigh number based on diameter was in the range $10^8 < Ra < 10^{10}$. It was concluded that in this range the natural convection mechanism departs considerably from the pattern known in the limit $Ra \to 0$. Specifically, the end-to-end heat transfer is effected via two thin horizontal jets, the upper (warm) jet proceeding along the top of the cylinder toward the cold end and the lower (cold) jet advancing along the bottom in the opposite direction. The region sandwiched between the two jets is filled with nearly stagnant fluid. In this region the temperature varies linearly with depth. In each vertical cross-section, the top-bottom temperature difference is of the same order of magnitude as the end-to-end temperature difference. The Nusselt number for end-to-end heat transfer was shown to vary weakly with the Rayleigh number.

NOMENCLATURE

- A_0, cross-sectional area of tube [m^2];
- A, function of Reynolds number [equation (1)];
- B, function of Reynolds number [equation (1)];
- D_0, diameter of tube [m];
- D, diameter of wire velocity probe [m];
- g, gravitational acceleration [$m\,s^{-2}$];
- K_1, the radius/length ratio [equation (6)];
- k, thermal conductivity [$W\,m^{-1}\,K$];
- L, cavity length [m];
- Nu, Nusselt number [equation (4)];
- Q, net heat transfer rate [W] [equation (4)];
- Ra, Rayleigh number based on diameter [equation (5)];
- Re, Reynolds number [equation (2)];
- T_H, warm end temperature [K];
- T_L, cold end temperature [K];
- ΔT, temperature difference between warm end and cold end [K];
- Δt, elapsed time [s];
- U_{app}, apparent velocity [$m\,s^{-1}$] [equation (1)];
- U_∞, free stream velocity [$m\,s^{-1}$];
- Δx, streak length [m].

Greek symbols

- α, thermal diffusivity [$m^2\,s^{-1}$];
- β, coefficient of volumetric thermal expansion [K^{-1}];
- ν, kinematic viscosity [$m^2 s^{-1}$].

INTRODUCTION

IN A 1977 paper, Hong [1] reported results from a numerical study of natural convection in a horizontal pipe with different end-temperatures and zero net mass flow. He was able to show that the end-to-end heat transfer is effected via a longitudinal counterflow which fills the entire pipe cross-section: the upper half of the cross-section is filled with warm fluid proceeding toward the cold end, while cold fluid returns toward the warm end through the bottom half of the cross-section. One consequence of this counterflow is the temperature variation around the pipe circumference, the upper side of the pipe being warmer than the lower side. The wall thermal stresses due to the flow-induced circumferential temperature variation are known to be a real problem in the design of nuclear reactor piping.

In a more recent paper Bejan and Tien [2] studied the same phenomenon theoretically using a perturbation analysis valid for small Rayleigh numbers. Their theory verified the main flow features first described by Hong [1], also pointing out some inconsistencies in Hong's work. For example, the pertubation analysis revealed a four-spiral secondary flow superimposed on the main horizontal counterflow. Furthermore, the circumferential temperature distribution predicted by Bejan and Tien was shown to differ by an order of magnitude from the distribution obtained numerically by Hong.

The objective of this paper is to describe what we think is the first *experimental* study of the natural convection phenomenon. In the experiment we simulated conditions (size, temperature difference) which are most likely to be present in a real application. As a result, the experimental study focused on the high Rayleigh number range $10^8 < Ra < 10^{10}$. The experimental results outlined below demonstrate conclusively that the flow and heat-transfer mechanisms differ fundamentally from the $Ra \to 0$ picture painted in the available literature [1, 2].

EXPERIMENT APPARATUS

The apparatus is a plexiglass tube shown in the scale

drawing of Fig. 1. The main feature of the apparatus is a horizontal cylindrical cavity of length $L = 124.5$ cm (49 in.) and diameter $D_0 = 14$ cm (5.5 in.). The geometry aspect ratio is therefore $D/L = 0.112$. The plexiglass wall thickness is 6.4 mm ($\frac{1}{4}$ in.). Throughout the experiment, the plexiglass tube was wrapped in a fibreglass wool blanket 10 cm thick. The two ends of the plexiglass tube were constructed out of aluminum plate with a thickness of 1.3 cm ($\frac{1}{2}$ in.). The two end-discs were epoxied in place, and the outer (visible) portion of the seal was reinforced with silicone rubber. We found that this simple design performed very well, particularly in view of the fact that metal–plexiglass seals are notorious for leaks in large scale structures exposed to significant temperature excursions.

The warm end of the cylindrical cavity was heated with an electric disc heater (300 W maximum) clamped tightly against the aluminum plate. The exposed part of the warm end was covered with a plexiglass cup filled with fiberglass insulation. The opposite end of the tube was cooled with running water circulated through a disc-shaped jacket soldered onto the back of the aluminum plate. The temperature and velocity measurements reported here were carried out through nine access ports positioned as shown in Fig. 1. The ports are labeled A through D, port A being the closest to the warm end. Each port is connected to a vertical plexiglass tube which has an I.D. of 0.3 cm ($\frac{1}{8}$ in.).

The experiments were performed using distilled water in the cylindrical cavity. A number of steady states were achieved by varying the electric heat input to the warm end and keeping the cold end at a constant temperature. One problem we had to overcome was posed by fluctuations encountered in the voltage supplied to the electric heater. We successfully reduced these fluctuations to less than ± 0.3°C by installing a constant-voltage transformer between the building voltage supply and the heater. There were also temperature fluctuations of ± 1°C in the cooling water circulated through the cold end jacket. However, these fluctuations had a period of 24 h which is about five times the characteristic response time of the apparatus (5 h). Consequently, the cold water temperature excursion was tolerated in the experiment.

TEMPERATURE MEASUREMENTS

The temperature field inside the horizontal cylindrical cavity was probed using a 2 KΩ bead-in-glass thermistor with a 0.3 mm bead dia. The thermistor was mounted at the end of a stiff stainless steel capillary tube which was lowered to any desired depth through each of the nine access ports. The thermistor resistance was measured with a digital ohmmeter, yielding temperature measurements accurate within ± 0.1°C.

Representative temperature results are reported in Figs. 2, 3, and 4a, b. Figure 2 shows the temperature-depth variation under each access port, for one of the lowest Rayleigh numbers achieved in this experiment, $Ra = 2.44 \times 10^8$. Figure 3 shows the same set of measurements this time for one of the highest Rayleigh numbers, $Ra = 8.63 \times 10^9$. To these authors' knowledge, this is the highest Rayleigh number (based on the vertical dimension) studied experimentally in connection with natural convection in horizontal enclosures with different end-temperatures, higher than $Ra = 8.11 \times 10^8$ reached by Imberger [3], also higher than $Ra = 1.59 \times 10^9$ reported recently by Al-Homoud and Bejan [4]. Finally, Figs. 4a, b, illustrate the variation with longitudinal position of the top, mid-depth and bottom temperatures in the vertical rectangular section cut through the cylinder axis.

The basic feature of the temperature field is the presence of a stratified core (inner, mid-depth, region) which covers almost the entire vertical diameter. In the stratified region the temperature varies almost linearly in the vertical direction and it is practically independent of longitudinal position. As shown by measurements at stations C_1 and C_2, the linearly stratified mid-depth region extends unchanged in the direction perpendicular to the plane of Fig. 1. Overall,

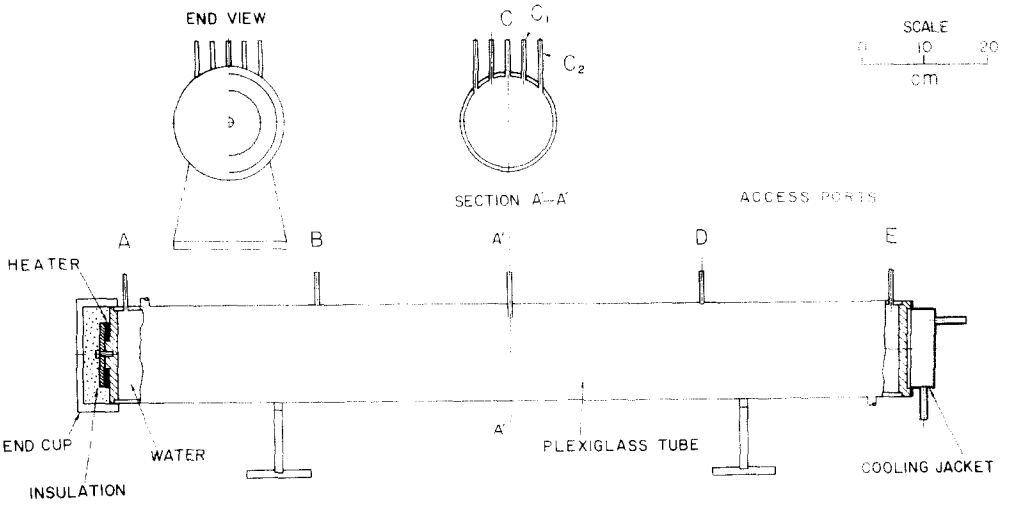

FIG. 1. Schematic of experimental apparatus.

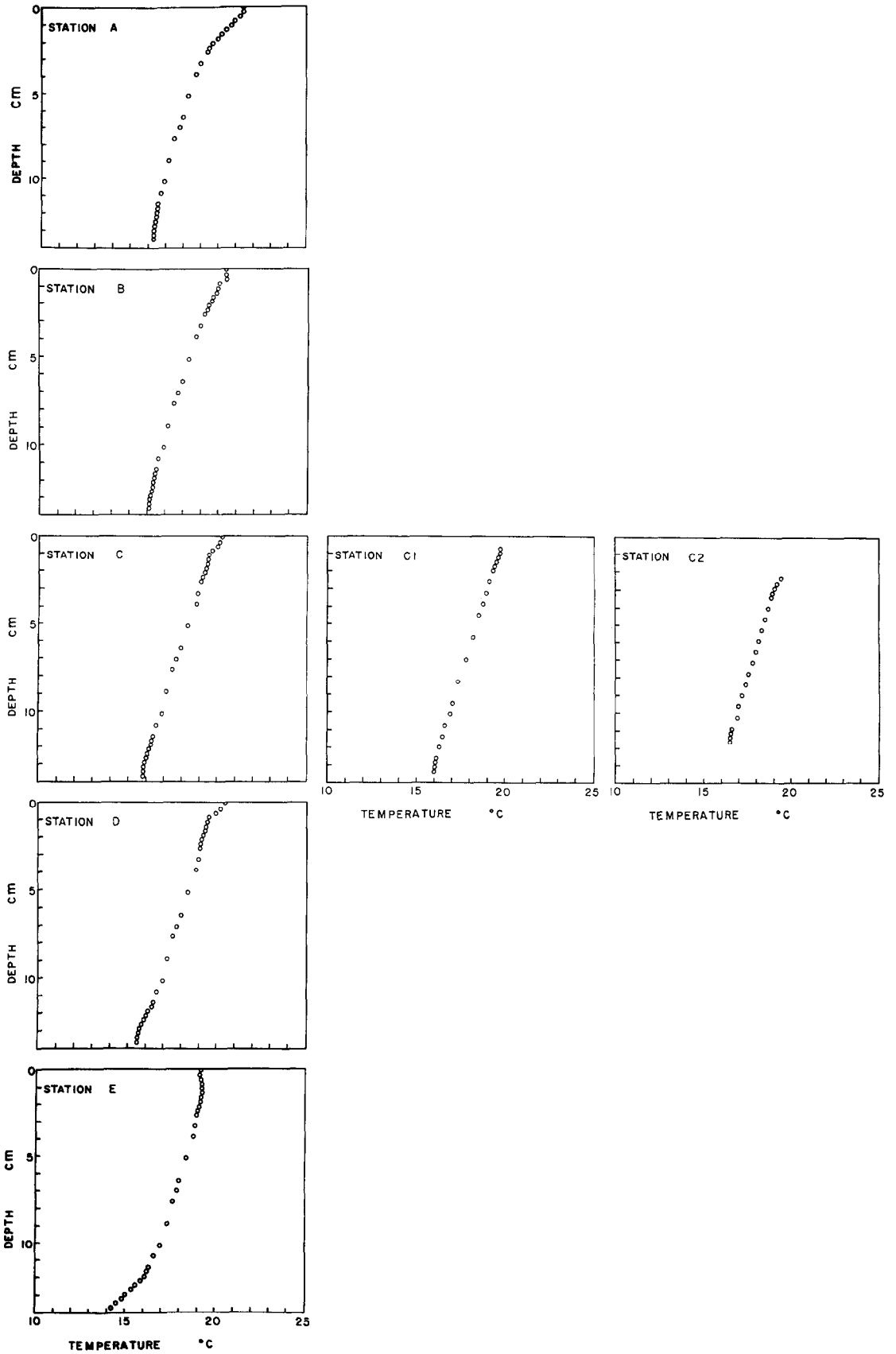

FIG. 2. Temperature distribution along the vertical diameter, $Ra = 2.44 \times 10^8$.

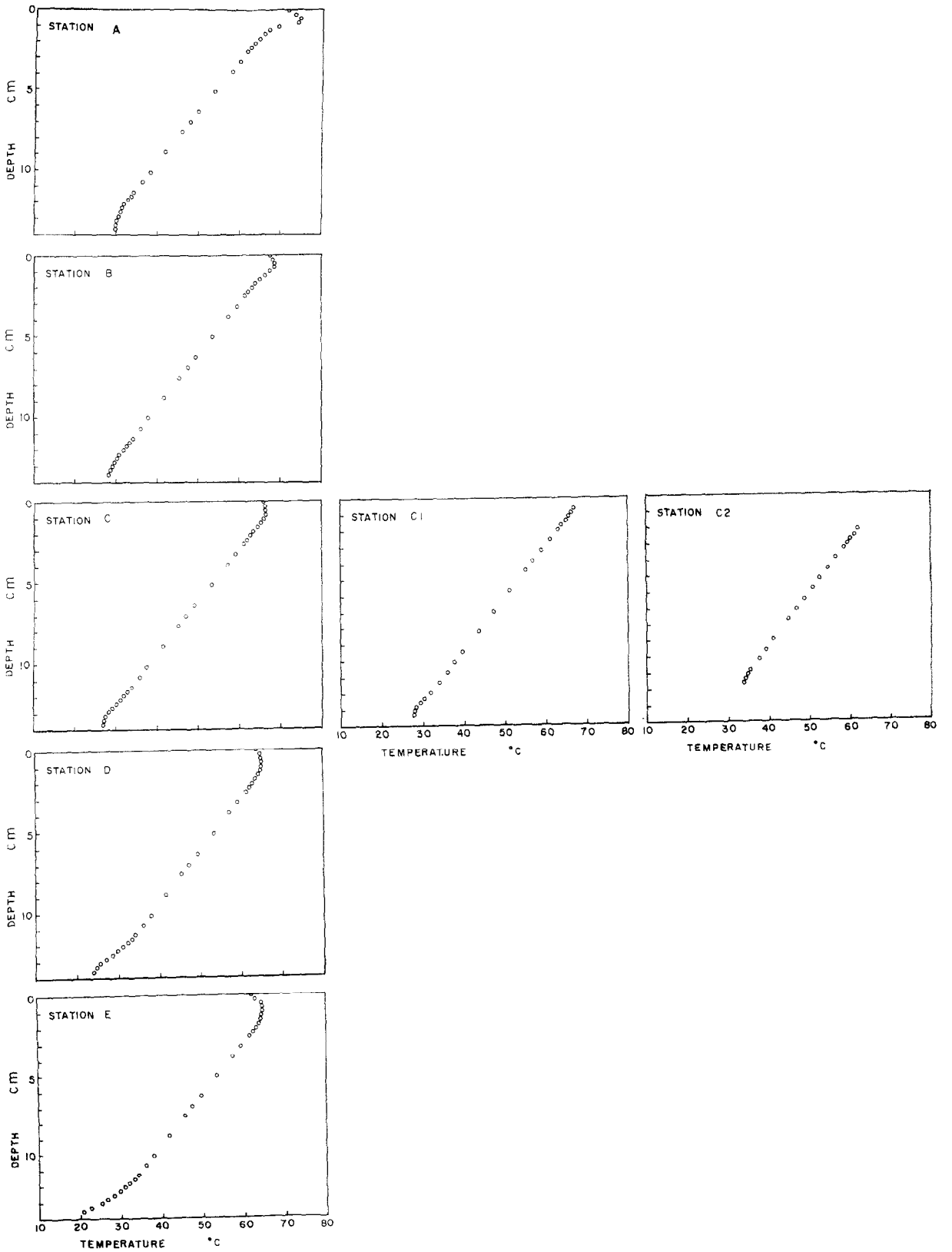

FIG. 3. Temperature distribution along the vertical diameter, $Ra = 8.63 \times 10^9$.

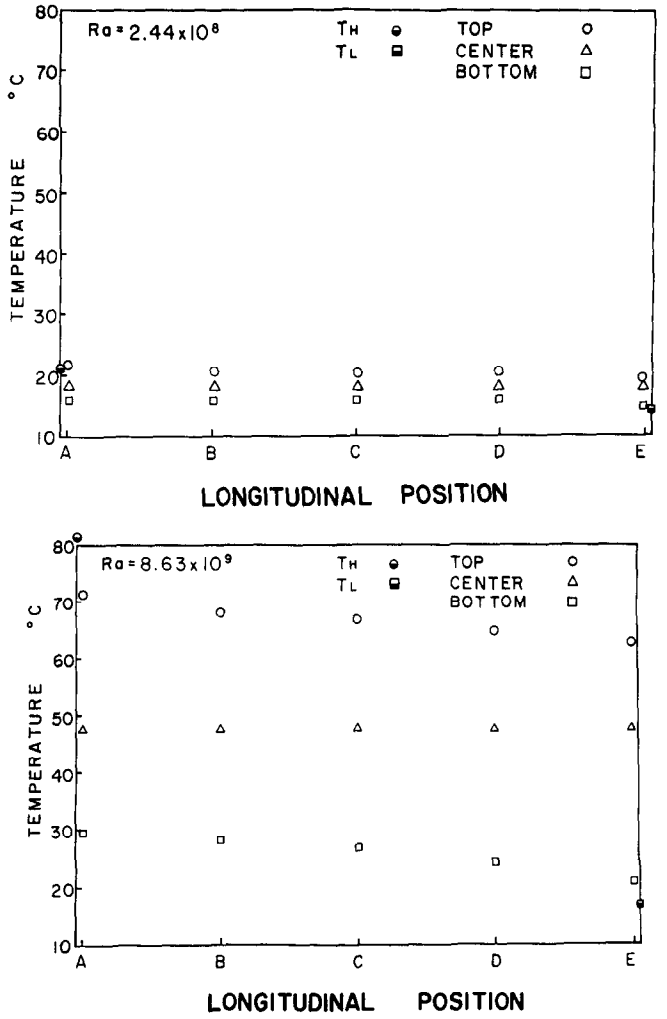

FIG. 4. Top, center and bottom temperature variation with longitudinal position, (a) $Ra = 2.44 \times 10^8$, (b) 8.63×10^9.

the vertical temperature gradient in the inner region increases with the Rayleigh number, i.e. from Fig. 2 to Fig. 3.

Near the top and bottom of the horizontal cavity the temperature distribution departs significantly from the linear distribution present in the mid-depth region. As demonstrated by the flow visualization experiments reported in the next section, the nonlinear top and bottom extremities of the vertical temperature profile are a reflection of horizontal jet flow. In addition to a strongly non-linear variation in the vertical direction (across the jet), the jet-layer temperature shows a variation with longitudinal position (Fig. 4a, b).

In conclusion, the temperature field differs fundamentally from the field determined numerically by Hong [1] and analytically by Bejan and Tien [2]. The difference is due to the fact that in the present experiment the Rayleigh number is considerably higher than in the low *Ra* limit considered in [1 and 2] in which the natural counterflow was modeled as *fully-developed* (without a linearly stratified mid-depth region).

VELOCITY MEASUREMENTS AND FLOW VISUALIZATION

Velocity measurements were made using the pH indicator (thymol blue) technique first described by Baker [5]. This technique was used successfully in a number of natural convection experiments [3, 6–8]. In the present experiment we lowered a vertical stainless steel wire (welding rod, 0.8 mm dia.) through each access port. We then applied 6V between the wire (cathode) and the nearest aluminum end-plate. As shown in Figs. 5 and 6, the vertical wire generated dark equidistant streaks in the water–thymol blue solution. The equidistant streaks were the result of painting the wire with Varathane ® over sections 4.8 mm long leaving exposed sections 1.2 mm long in between.

The velocity measurements were based on photographing the streak pattern, at the same time recording the time elapsed in the development of the pattern. However, at a given depth, the local velocity is not equal to the streak length Δx divided by the time interval Δt. As pointed out by Imberger [3, 9], the difficulty with the thymol blue method is that the blue

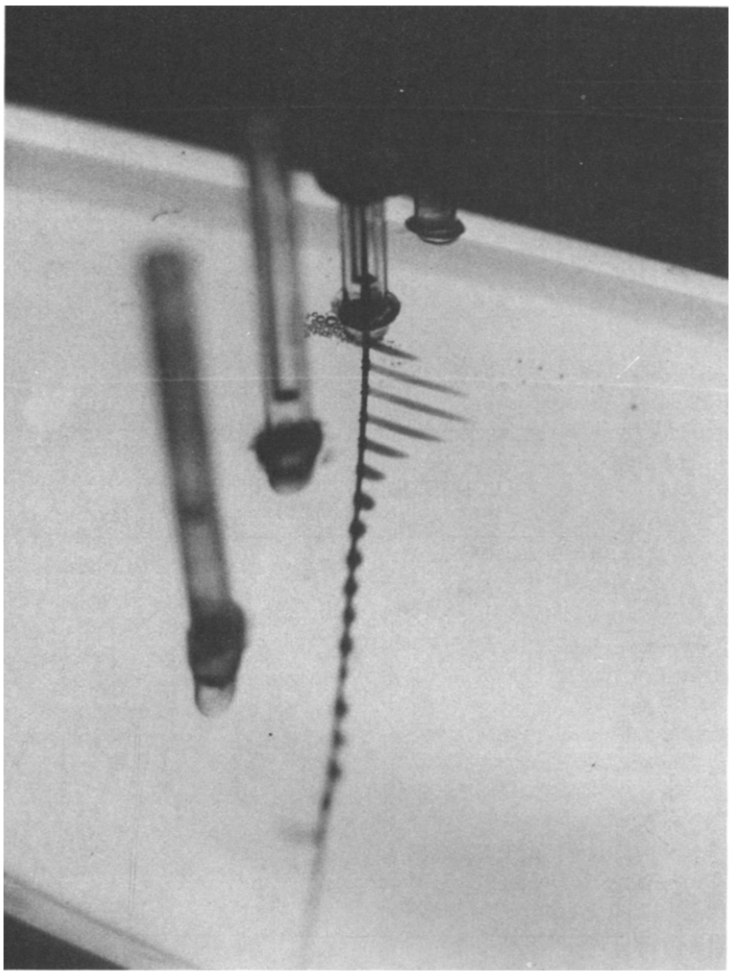

FIG. 5. Streak pattern of top jet at access port C, $Ra = 3.09 \times 10^8$, $\Delta t = 62.16$ s.

dye is generated in a thin layer around the wire and then swept into the wake of the wire. The dye is only slowly released from the wake into the free stream whose velocity U_∞ is to be measured. Therefore, the free stream velocity cannot be assumed equal to the 'apparent' velocity $U_{app} = \Delta x/\Delta t$.

With the above argument in mind, we found it necessary to calibrate the velocity probe. We towed the actual wire at known speed (U_∞) through a tank filled with stagnant thymol blue solution. In the laboratory, it was easier to run the towing in reverse, by placing the tank on the slow-moving table of a *quiet* milling machine and by holding the vertical wire in the chuck. For each run (U_∞) we took a sequence of approximately six photographs (sets Δx, Δt). As shown in Fig. 7, the results are correlated reasonably well by the expression

$$\frac{U_{app}}{U_\infty} = 1 - Ae^{-B(\Delta x/D)} \tag{1}$$

where D is the wire diameter, Δx the distance behind the wire and A, B empirical functions of Reynolds number $Re = U_\infty D/\nu$,

$$A = 0.84\,Re^{0.10} \tag{2}$$

$$b = 0.029\,Re^{0.11} \tag{3}$$

With Δx, D and $U_{app} = \Delta x/\Delta t$ known from each photograph, the local free stream velocity U_∞ follows from equation (1) using an iterative procedure. The calculation is a tedious one, particularly since one must take into account the variation of viscosity (ν) with temperature from streak to streak along the wire. Figure 8 shows the resulting velocity profiles at stations B, C, D for an intermediate Rayleigh number, $Ra = 1.78 \times 10^9$. Each velocity profile was calculated from a set of three photographs taken from different angles in order to record the entire streak pattern. As shown in Figs. 5 and 6, in each photograph the extremities of the streak pattern are invisible due to the curvature of the apparatus.

In the central portion of the pipe the flow consists of two thin jets, one flowing toward the cold end along the top line and the other flowing in the opposite direction along the bottom. In both jets, the fluid decelerates in the direction of flow. Due to the viscosity–temperature variation in the vertical direction, velocities in the warm (upper) jet are noticeably higher than in the cold (lower) jet.

In the mid-depth region the fluid is practically

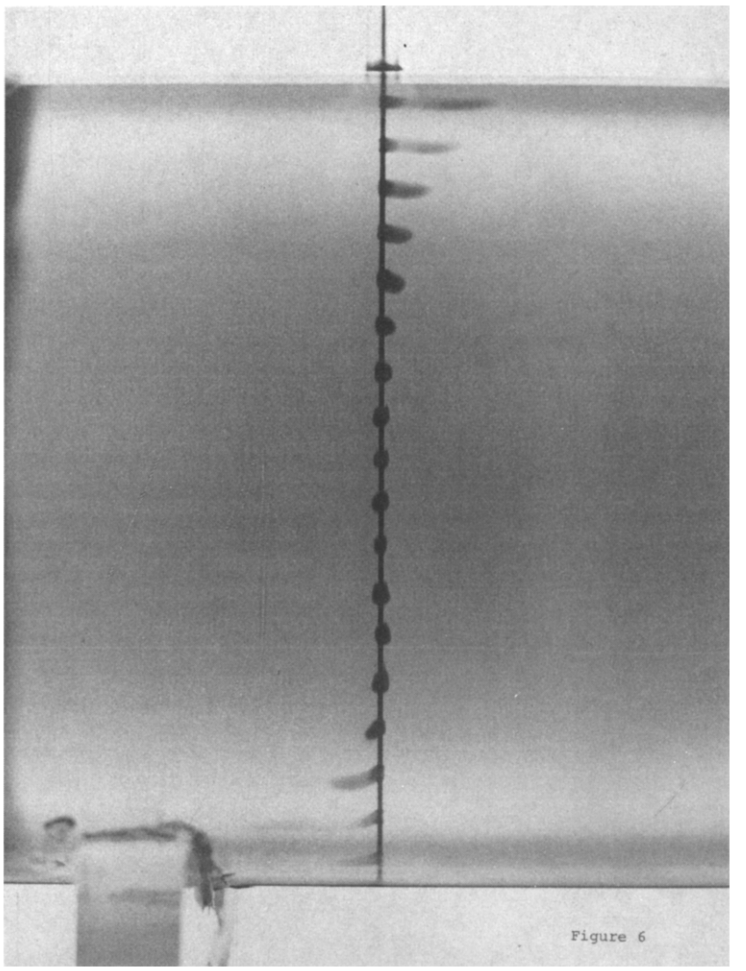

FIG. 6. Streak pattern of core region at access port B, $Ra = 3.09 \times 10^8$, $\Delta t = 62.46$ s.

stagnant. Figure 8 suggests that a very weak clockwise counterflow may persist at mid-depth where, as shown in the preceding section, the fluid is thermally stratified. Streak patterns photographed at stations C_1 and C_2 (not shown) demonstrate that the nearly stagnant region extends laterally without any visible change in vertical dimension.

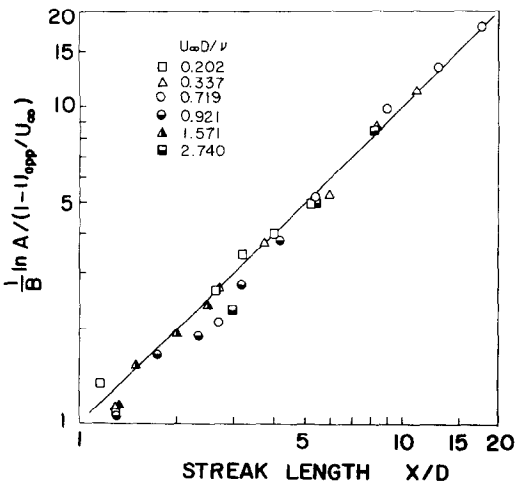

FIG. 7. Calibration curve for the velocity probe.

The lack of three-dimensional motion in the inner (mid-depth) region is explained by the fact that the temperature varies only with depth. Therefore, in the mid-depth region of the pipe cross-section the isotherms are horizontal, i.e. almost perpendicular to the wall (in agreement with the adiabatic wall condition). Since the isotherms must also be perpendicular to wall in the upper and lower portions of the pipe cross-section, we expected to detect a spiraling secondary flow concentrated in the two jet regions. To the best of our technique we could not detect three-dimensional motion in the extreme regions. We feel that the further study of such effects requires an apparatus with more than two transverse access ports (C_1, C_2).

In conclusion, we demonstrated that in the range $Ra = 10^8$–10^{10} the flow pattern differs fundamentally from the pattern known previously [1, 2]. In the earlier studies the counterflow was envisioned as fully developed; this counterflow would appear in Fig. 8 as S-shaped velocity profiles independent of longitudinal position. Using Fig. 8, it can be argued that if the Rayleigh number were to decrease from the present level toward the $Ra \to 0$ limit of [1, 2], the jets would gradually slow down and grow vertically. This process

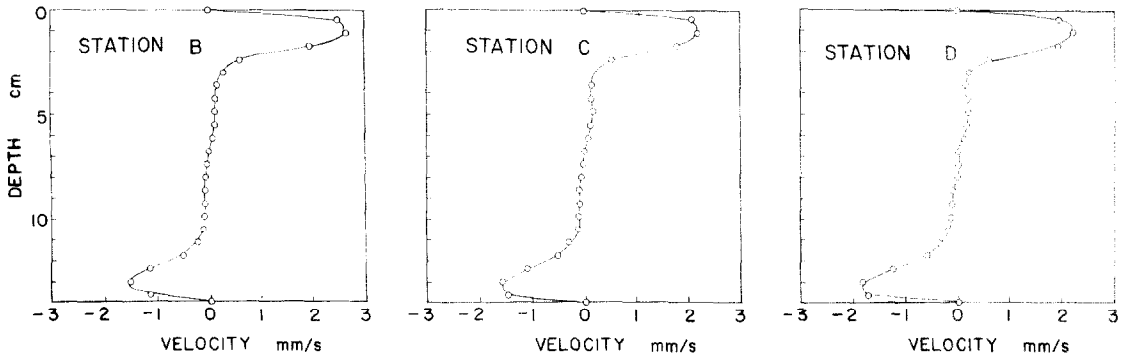

FIG. 8. Velocity distribution at stations B, C and D; $Ra = 1.78 \times 10^9$.

would eventually eliminate the stagnant mid-depth region, yielding fully-developed S-shaped profiles as in [1,2].

HEAT TRANSFER RESULTS

The net transfer rate in the longitudinal direction through the horizontal pipe was measured experimentally. The results are summarized in Fig. 9 as a plot of Nusselt number vs Rayleigh number,

$$Nu = \frac{Q}{kA_0\Delta T/L} \tag{4}$$

$$Ra = \frac{g\beta D_0^3 \Delta T}{\alpha \nu} \tag{5}$$

In the above definitions, Q, D_0, A_0 and ΔT are the net heat transfer rate (W), pipe diameter, tube cross-sectional area and end-to-end temperature difference, respectively. The physical properties appearing in

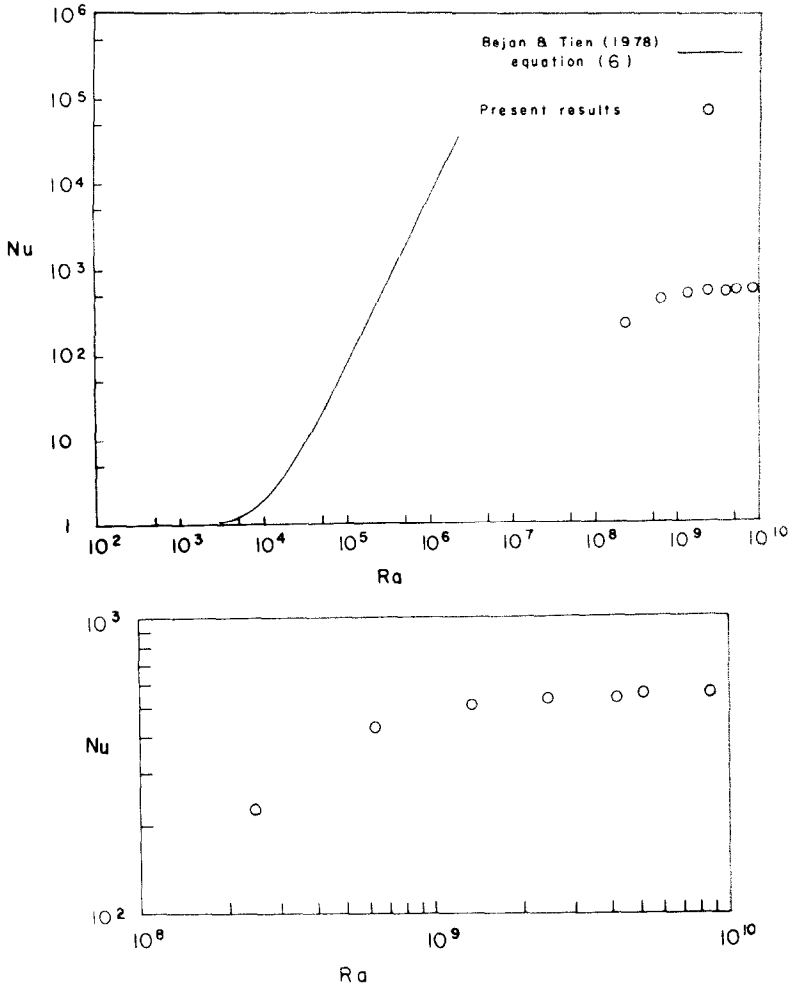

FIG. 9. Summary of heat-transfer measurements.

expressions (4) and (5) are defined in the Nomenclature.

For each steady state achieved in the apparatus we measured the end-plate temperatures using thermistors imbedded in the center of each plate. The physical properties appearing in the definitions of Nu and Ra were evaluated at the arithmetic mean temperature of the two ends.

The heat transfer rate Q was measured electrically, by recording the voltage across and current through the warm end heater. Before substituting this quantity in the Nusselt number definition (4), we ran a full-size experiment to determine the actual heat leak from the apparatus with no cooling water supplied to the cold end jacket [10]. A succession of steady states were achieved by dissipating a small number of Watts in the warm end heater. This heat input was balanced by the leakage of heat across the fiberglass insulation packed around the apparatus. The object of the experiment was to reproduce an apparatus–ambient temperature difference comparable with the difference recorded during actual experiments. The heat leak experiment provided a quantitative, albeit approximate, estimate of the heat leak for a known temperature difference. Using this method we found that the heat leak is indeed minimal, reaching a maximum of 7% in the case of maximum heating rate supplied by the electric heater (300 W). In conclusion, for most of the data assembled in Fig. 9 the power supplied electrically to the end heater is convected horizontally through the pipe and reaches the cold end nearly intact.

The heat transfer results assembled in Fig. 9 provide additional evidence that at high Ra the heat transfer mechanism differs greatly from the fully-developed counterflow known previously. Next to our results we show the Nusselt number predicted with the Bejan and Tien theory [2]

$$Nu = 1 + \frac{7}{2949120}(K_1 Ra)^2 \qquad (6)$$

were K_1 is the radius/length ratio, $K_1 = 0.056$. Our results show that in the range $Ra = 10^8$–10^{10} the Nusselt number dependence on Ra is considerably weaker than in the $Ra \to 0$ limit. This conclusion is qualitatively similar to recent findings regarding overall heat transfer in two-dimensional horizontal enclosures at high Rayleigh number [4].

CONCLUSIONS

In this article we reported representative results from what we see as the first experimental study of natural convection in a horizontal pipe heated in the end-to-end direction. We demonstrated that in the Rayleigh number range $10^8 < Ra < 10^{10}$ the heat transfer mechanism and the fluid mechanics of the phenomenon differ fundamentally from the mechanism thought to prevail in the $Ra \to 0$ limit [1, 2]. The experimental results enabled us to point out the following new features:

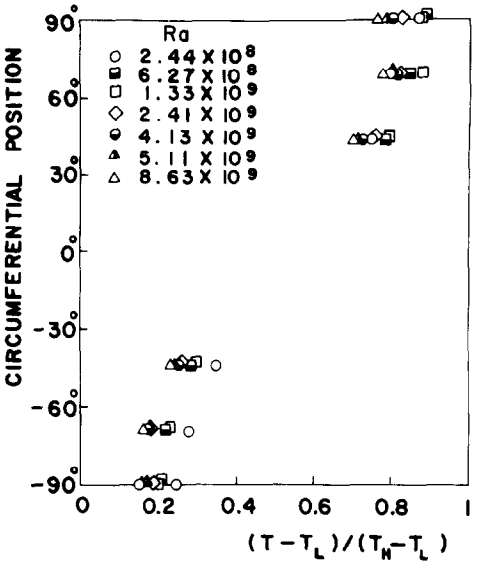

FIG. 10. Circumferential temperature distribution around the mid-section.

1. The natural circulation in the pipe is effected via two thin jets running in counterflow. The warm jet advances toward the cold end along the top line of the cylindrical cavity, while the cold jet flows in the opposite direction along the bottom.

2. Most of the pipe volume sandwiched between the two jets is occupied by nearly stagnant fluid. The temperature in this 'mid-depth' region varies linearly with depth and is practically uniform in any given horizontal plane (at points not too close to the vertical end-walls).

3. The overall Nusselt number for end-to-end heat transfer through the pipe shows a relatively weak dependence on Rayleigh number. The net heat transfer rate differs greatly from estimates based on available theoretical results such as the theory given in [2]. We also expect the Nusselt number to depend on the aspect ratio D_0/L. Unfortunately, in our experimental study D_0/L was fixed by the apparatus, and a systematic evaluation of the effect of D_0/L on Nu was not possible. Some understanding of the role played by D_0/L may be gained from comparing the present measurements with those made by Elder [11] in a tall rectangular cavity. We would expect Elder's results to agree approximately with the picture in a short horizontal cylinder ($D_0/L > 1$).

Finally, in Fig. 10 we present the circumferential temperature distribution in the middle of the pipe. As pointed out by Hong [1], this information is relevant to the thermal stress analysis of piping systems encountered in nuclear reactor engineering. It is clear that at high Ra the top-to-bottom temperature difference is of the same order of magnitude as the end-to-end temperature difference. Of engineering significance is the fact that when the Rayleigh number is high enough, the temperature variation induced around the pipe circumference does not depend on the length of the pipe.

Acknowledgement—This research was supported by the National Science Foundation through Grant No. ENG 78-20957. We thank Mr. Karl Rupp and Mr. Richard Cowgill for their contributions in this experimental project.

REFERENCES

1. S. W. Hong, Natural circulation in horizontal pipes, *Int. J. Heat Mass Transfer* **20,** 685–691 (1977).
2. A. Bejan and C. L. Tien, Fully developed natural counterflow in a long horizontal pipe with different end temperatures, *Int. J. Heat Transfer* **21,** 701–708 (1978).
3. J. Imberger, Natural convection in a shallow cavity with differentially heated end walls—3. Experimental results, *J. Fluid Mech.* **65,** 247–260 (1974).
4. A. A. Al-Homoud and A. Bejan, Experimental Study of high Rayleigh number convection in horizontal cavity with different end temperatures, Report CUMER-79-1, Department of Mechanical Engineering, University of Colorado, Boulder, (May 1979).
5. D. J. Baker, A technique for the precise measurement of small fluid velocities, *J. Fluid Mech.* **26,** 573–575 (1966).
6. M. Vedhanayagam, J. H. Lienhard and R. Eichhorn, Method for visualizing high Prandtl number heat convection, *J. Heat Transfer* **101,** 571–573 (1979).
7. E. M. Sparrow, R. B. Husar and R. J. Goldstein, Observations and other characteristics of thermals, *J. Fluid Mech.* **41,** 793–800 (1970).
8. R. Eichhorn, J. H. Lienhard and C. C. Chen, Natural convection from isothermal spheres and cylinders immersed in a stratified fluid, Paper NC 1.3, *Proc. 5th Int. Heat Transf. Conf.*, Tokyo (1974).
9. J. Imberger, Private communication (10 May, 1979).
10. E. M. Sparrow, Private communication (23 March 1979).
11. J. W. Elder, Laminar free convection in a vertical slot, *J. Fluid Mech.* **23,** 77–98 (1965).

ETUDE EXPERIMENTALE DE CONVECTION NATURELLE DANS UN CYLINDRE HORIZONTAL AVEC DES TEMPERATURES DIFFERENTES AUX EXTREMITIES

Résumé—Le phénomène de convection naturelle dans un tube horizontal avec différentes températures d'extrémité est étudié expérimentalement dans une cavité cylindrique avec un rapport diamètre/longueur égal à 0,112. Le nombre de Rayleigh basé sur le diamètre varie tel que $10^8 < Ra < 10^{10}$. Dans ce domaine, la convection naturelle diffère considérablement de la configuration connue pour la limite $Ra \to 0$. Spécifiquement le transfert thermique d'une extrémité à l'autre se fait par deux courants horizontaux minces, le courant supérieur (chaud) avançant le long du sommet du cylindre vers l'extrémité froide, le courant inférieur (froid) se déplaçant dans la direction opposée. La région entre ces deux courants correspond à du fluide immobile Dans cette région la température varie linéairement avec la profondeur. Dans toute section droite verticale, la différence de température entre haut et bas est du même ordre de grandeur que la différence de température entre les extrémités. Le nombre de Nusselt pour le transfert entre extrémités varie faiblement avec le nombre de Rayleigh.

EXPERIMENTELLE UNTERSUCHUNG DER FREIEN KONVEKTION IN EINEM HORIZONTALEN ZYLINDER MIT VERSCHIEDENEN ENDTEMPERATUREN

Zusammenfassung—Das Phänomen der freien Konvektion in einem horizontalen Rohr mit verschiedenen Endtemperaturen wurde experimentell in einem zylindrischen Hohlraum mit dem Verhältnis (Durchmesser)—(Länge) = 0,112 untersucht. Die Rayleigh-Zahl, bezogen auf den Durchmesser, lag im Bereich $10^8 < Ra < 10^{10}$. Es wurde festgestellt, daß in diesem Bereich der Mechanismus der freien Konvektion stark von dem für den Grenzfall $Ra \to 0$ bekannten Muster abweicht. Insbesondere wird der Wärmetransport von Ende zu Ende durch zwei dünne horizontalle Strahlen bewirkt, dem oberen (warmen) Strahl, der oben am Zylinder entlang zum kalten Ende strömt und dem unteren (kalten) Strahl, der sich an der Unterseite in umgekehrter Richtung bewegt. Das zwischen den beiden Strahlen gelegene Gebiet ist von nahezu ruhendem Fluid gefüllt. In diesem Gebiet verändert sich die Temperatur linear mit der Tiefe. In jedem vertikalen Querschnitt ist die Temperaturdifferenz zwischen oben und unten von gleicher Größenordnung wie die Temperaturdifferenz von Ende zu Ende. Es wurde gezeigt, daß die Nusselt-Zahl für den Wärmetransport von Ende zu Ende sich leicht mit der Rayleigh-Zahl verändert.

ЭКСПЕРИМЕНТАЛЬНОЕ ИССЛЕДОВАНИЕ ЕСТЕСТВЕННОЙ КОНВЕКЦИИ В ГОРИЗОНТАЛЬНОМ ЦИЛИНДРЕ С РАЗЛИЧНОЙ ТЕМПЕРАТУРОЙ НА ТОРЦАХ

Аннотация — Проведено экспериментальное исследование естественной конвекции в горизонтальной трубе с различной температурой на торцах при отношении диаметра к длине цилиндра, равном 0,112. Число Релея, отнесенное к диаметру, изменялось в диапазоне от 10^8 до 10^{10}. Найдено, что в этом диапазоне механизм естественной конвекции существенно отличается от механизма, имеющего место в пределе $Ra \to 0$. В частности, перенос тепла от торца к торцу осуществляется посредством двух тонких горизонтальных струй, причем верхняя (нагретая) струя движется в верхней части цилиндра в сторону холодного торца, а нижняя (холодная) струя — в нижней части в противоположном направлении. Область между двумя струями заполнена почти неподвижной жидкостью, в которой температура изменяется линейно по глубине. В каждом поперечном сечении разность температур по вертикали между верхней и нижней частями цилиндра является того же порядка величины, что и разность температур между торцами. Показано, что число Нуссельта для теплопереноса от торца к торцу слабо изменяется с изменением числа Релея.